Synthesis and Characterization of the Mixed-valence $[Fe^{II}Fe^{III}BPLNP(OAc)_2](BPh_4)_2$ Complex As a Model for the Reduced Form of the Purple Acid Phosphatase

Jeseung Lee, Dong J. Jung, Ho-Jin Lee, Kang-Bong Lee,† Nam Hwi Hur,‡ and Ho G. Jang*

Department of Chemistry, Division of Chemistry and Molecular Engineering, Korea University, Seoul 136-701, Korea
†Advanced Analysis Center, KIST, Seoul 136-130, Korea
‡Korea Research Institute of Standards and Science, Taejon 305-600, Korea
Received July 25, 2000

$[Fe^{II}Fe^{III}BPLNP(OAc)_2](BPh_4)_2$ (**1**), a new model for the reduced form of the purple acid phosphatases, has been synthesized by using a dinucleating ligand, 2,6-bis[((2-pyridylmethyl)(6-methyl-2-pyridylmethyl)amino)methyl]-4-nitrophenol (HBPLNP). Complex **1** has been studied by electronic spectral, NMR, EPR, SQUID, and electrochemical methods. Complex **1** exhibits two strong bands at 498 nm ($\varepsilon = 2.6 \times 10^3$ $M^{-1}cm^{-1}$) and 1363 nm ($\varepsilon = 5.7 \times 10^2$ $M^{-1}cm^{-1}$) in CH_3CN. These are assigned to phenolate-to-Fe^{III} and intervalence charge-transfer transitions, respectively. NMR spectrum of complex **1** exhibits sharp isotropically shifted resonances, which number is half of those expected for a valence-trapped species, indicating that electron transfer between Fe^{II} and Fe^{III} centers is faster than NMR time scale at room temperature. Complex **1** undergoes quasireversible one-electron redox processes. The $Fe^{III}{}_2/Fe^{II}Fe^{III}$ and $Fe^{II}Fe^{III}/Fe^{II}{}_2$ redox couples are at 0.807 and 0.167 V versus SCE, respectively. It has $K_{comp} = 5.9 \times 10^{10}$ representing that BPLNP/bis(acetato) ligand combination stabilizes a mixed-valence $Fe^{II}Fe^{III}$ complex in the air. Interestingly, complex **1** exhibits intense EPR signals at g = 8.56, 5.45, 4.30 corresponding to mononuclear high-spin Fe^{III} species, which suggest a very weak magnetic coupling between the iron centers. Magnetic susceptibility study shows that there is a very weak antiferromagnetic coupling (J = -0.78 cm^{-1}, $\boldsymbol{H} = -2JS_1 \cdot S_2$) between Fe^{II} and Fe^{III} centers. Thus, we can suggest that complex **1** has a very weak antiferromagnetic coupling between the iron centers due to the electronic effect of the nitro group in the bridging phenolate ligand.

Introduction

The purple acid phosphatases (PAP) constitute to a novel class of non-heme metalloenzymes that catalyze the hydrolysis of various phosphate esters under weak acidic condition.[1] Although they have been isolated from a variety of mammalian, plant, and microbial sources, only the PAP enzymes isolated from bovine spleen (BSPAP),[2-8] porcine uterus (uteroferrin),[9-17] and red kidney been (KBPAP)[18,19] have been studied in some detail. Recently, a X-ray structure of the KBPAP was reported having a heteronuclear FeZn unit in the active site.[18] However, the active sites of most PAPs contain dinuclear iron centers with two accessible oxidation states: a reduced $Fe^{II}Fe^{III}$ form (PAP_{red}) and an oxidized $Fe^{III}Fe^{III}$ form (PAP_{ox}).[1] The catalytically active $Fe^{II}Fe^{III}$ form is pink (λ_{max} = 510 nm, ε = 4000 $M^{-1}cm^{-1}$), while the inactive $Fe^{III}Fe^{III}$ form is purple (λ_{max} = 560 nm, ε = 4000 $M^{-1}cm^{-1}$).[4,9-11] These bands are assigned as tyrosinate-to-Fe^{III} charge transfer transitions which are confirmed by Resonance Raman study.[5]

The reduced form of uteroferrin (Uf_{red}) exhibits rhombic EPR signals at g = 1.94, 1.73, and 1.58, which is consistent with an antiferromagnetically coupled high-spin Fe^{II} and Fe^{III} center.[6,11,12] In fact, magnetic susceptibility study shows that the Fe^{II} and Fe^{III} center is weakly antiferromagnetically coupled with J values ranging from -5 to -11 cm^{-1} (where, $\boldsymbol{H} = -2JS_1 \cdot S_2$).[5,14] When the phosphate binds to Uf_{red}, EPR signal intensity of $Uf_{red} \cdot PO_4$ diminishes, which is also consistent with a weaker antiferromagnetic coupling ($J \approx$ -3.0 cm^{-1}) for $Uf_{red} \cdot PO_4$.[12] Recent magnetic susceptibility study of the $Fe^{III}Fe^{III}$ form (Uf_{ox}) reveals a weak antiferromagnetic coupling ($J >$ -15 cm^{-1}), which indicates lack of μ-oxo bridge.[8] Unfortunately, X-ray structure and analysis has not been reported for the diiron PAP enzymes. However, EXAFS[7,15] and NMR[16] studies suggest that the iron center has an oxygen-rich coordination environment similar to that in ribonucleotide reductase.[20] It has also been suggested that iron centers are bonded to 3.5 N/O donors at about 2.14 Å, which are likely associated with histidine and aspartate or glutamate as well as a water molecule. A bridging hydroxo ligand has been suggested in the reduced form of the PAPs, but some controversy still exists on the nature of the bridging ligands in the oxidized form.

A number of recent model studies focused on the preparation of phenoxo-containing multidentate ligands having pyridine,[21,22] pyridine-lutidine,[23] imidazole,[24] benzimidazole,[25] carboxylate,[26] and pyridine-phenolate[27-31] as pendant arms. However, it is still very important to investigate the controlling factor of stabilization of mixed-valence states and the characterization of the physical properties of mixed-valence complexes.

In this study, we have approached the subtle change in the structure by introducing the substituent to the dinucleating ligand and investigated the physical properties of the mixed-valence complex. We report the synthesis of the new dinucleating HBPLNP ligand and the spectral, electrochemical, and magnetic properties of the mixed-valence complex $[Fe^{II}Fe^{III}BPLNP(OAc)_2](BPh_4)_2$ (**1**) as a new model for the

reduced form of the purple acid phosphatases.

Experimental Section

All reagents and solvents were purchased from commercial sources and used as received. Solvents were of either reagent or spectroscopic grade and were dried by standard procedures prior to use. 2,6-bis(bromomethyl)-4-nitrophenol and (2-pyridylmethyl)(6-methyl-2-pyridylmethyl)amine (PLA) was prepared by following previously reported procedure.[21,23] Microanalysis was performed by Korean Basic Science Research Institute, Seoul.

2,6-bis[((2-Pyridylmethyl)(6-methyl-2-pyridylmethyl)-amino)methyl]-4-nitrophenol (HBPLNP): This ligand was synthesized by the literature method[22] with the following modification. Under N_2 atmosphere, a mixture of (2-pyridylmethyl)(6-methyl-2-pyridylmethyl)amine (4.3 g, 20 mmol) and triethylamine (3.0 mL, 20 mmol) in 20 mL THF was added dropwise to a stirred THF solution of 2,6-bis(bromomethyl)-4-nitrophenol (3.25 g, 10 mmol) at 0 °C. When the addition was completed, the mixture was allowed to warm to room temperature. After 3 days, the above mixture was filtered to remove the ammonium salt, and the filtrate was concentrated under reduced pressure. The residue was dissolved in 40 mL of water, and the product was extracted with three 40 mL portions of CH_2Cl_2. The extract was washed with brine, and dried over anhydrous $MgSO_4$. The crude product was purified by column chromatography (ethylacetate : ethanol = 1 : 1) to afford a yellow oil (70% yield). ^{1}H NMR (300 MHz, $CDCl_3$): 2.55 (s, 6H, lutidyl-*CH*$_3$), 3.84, 3.87, 3.90 (s, s, s, 4H, 4H, 4H, Ar-*CH*$_2$, lutidyl-*CH*$_2$, pyridyl-*CH*$_2$), 7.00, 7.16, 7.27, 7.50, 7.62, 8.51 (d, t, d, d + t, t, d, 2H, 2H, 2H, 4H, 2H, 2H, lutidyl-*H*s and pyridyl-*H*s). 8.20 (s, 2H, Ar-*H*s).

[Fe^{II}Fe^{III}BPLNP(OAc)$_2$](BPh$_4$)$_2$ (1): A solution of 0.15 g (0.25 mmol) of HBPLNP in 10 mL methanol was treated with a solution of 0.202 g (0.50 mmol) of $Fe(NO_3)_3 \cdot 9H_2O$ in 5 mL methanol to yield a reddish-brown solution. After 30 min stirring at room temperature, 0.063 g (0.77 mmol) sodium acetate was added to above solution. After 1 hour stirring at room temperature, metathesis with 0.194 g (0.57 mmol) of sodium tetraphenylborate resulted in the immediate precipitation of the reddish-brown product. The crude product was purified by the vapor diffusion of ether into the CH_3CN solution of complex **1**. FAB$^+$-Mass m/z: 1133.3. Anal. Calcd. for [Fe^{II}Fe^{III}BPLNP(OAc)$_2$](BPh$_4$)$_2$, $C_{86}H_{80}B_2Fe_2N_7O_7$: C, 70.90; H, 5.53; N, 6.73. Found: C, 70.53; H, 5.21; N, 6.87.

Physical Measurements. ^{1}H NMR spectra were obtained on Varian Mercury 300 and Unity plus 600 spectrometers. The paramagnetic ^{1}H NMR spectra were obtained using a 90° pulse with 16K data points. An inversion-recovery pulse sequence (180°-τ-90°-AQ) was used to obtain non-selective proton relaxation times (T_1). A typical magnitude ^{1}H-COSY spectrum was collected with 1024 data points in t_2 and 256 data points in t_1 with a band width of 10 kHz and a repetition time of < 0.2 s. A zero-degree shifted sine bell was applied in both dimensions and zero-filled to 2048 $t_2 \times 2048$ t_1 data points prior to Fourier transformation and symmetrization. In this study, cross signals from pairs of signals with < 1 ppm in a spectral width of ~30 ppm could be clearly recognized under proper processing procedures. Electronic spectra were measured on a Hewlett-Packard 8453 biochemical analysis UV/Visible spectrophotometer. Near-IR spectrum was recorded with Varian Cary 5G spectrophotometer. X-band EPR measurements were performed with Bruker ESP-300S spectrometer equipped with an Oxford liquid helium cryostat. Electrochemical studies were performed with a BAS 50W electrochemical analyzer (Biochemical Systems, Inc., West Lafayette, IN). All electrochemical experiments were done under argon at ambient temperature in CH_3CN solutions with 0.1 M tetrabutylammonium perchlorate as the supporting electrolyte. Cyclic voltammogram was obtained by using a three-component system consisting of a platinum net working electrode, a platinum wire auxiliary electrode, and a BAS Ag/Ag$^+$ or saturated calomel reference electrode

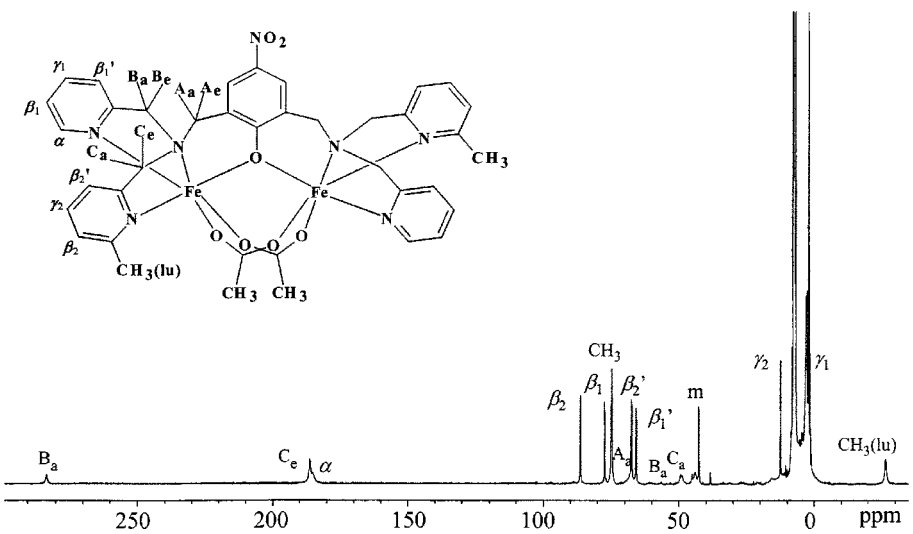

Figure 1. ^{1}H NMR spectrum of complex **1** in CD_3CN.

Table 1. Isotropic shifts and experimental relaxation times of complex **1**

Peak	Chemical shift (ppm)	T_{1exp} (ms)
$CH_2(A_a)$	68	
$CH_2(B_e)$	283	0.73
$CH_2(B_a)$	49	0.71
$CH_2(C_e)$	186	0.93
$CH_2(C_a)$	44	0.86
β_1	76	10.0
γ_1	1.8	31.5
β_1'	65	8.5
$CH_{3(lu)}$	-26	1.5
β_2	85	12.7
γ_2	12	21.5
β_2'	66	8.5
α	185	

Greek letters designate positions of pyridyl and lutidyl rings.

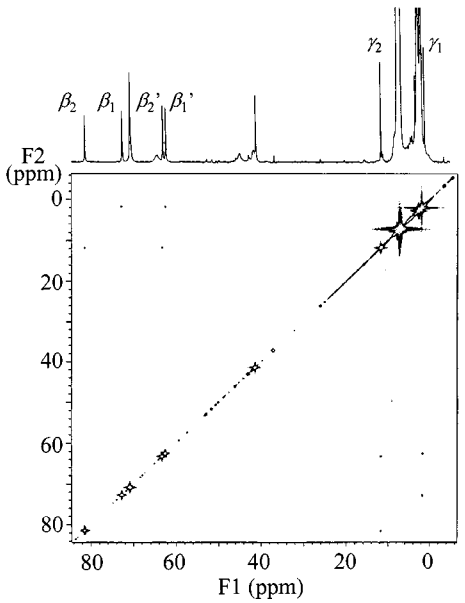

Figure 2. COSY spectrum of complex **1** in CD_3CN.

containing a vycor tip plug to separate it from the bulk solution. The ferrocenium/ferrocene couple was used to monitor the reference electrode.

Results and Discussion

^{1}H NMR studies. ^{1}H NMR spectroscopy has been established as a useful probe of the structural and magnetic properties of the mixed-valence complexes.[32] The NMR spectrum of complex **1** displays relatively sharp well-resolved resonances that span 350 ppm range in chemical shift. The narrow line widths of the signals are consistent with the diiron(II,III) complex adopting the T_{1e} of the fast electronic relaxation high-spin Fe^{II} center (Figure 1).[33] Most of protons are assigned by comparison of integration, T_1 values (Table 1), COSY connectivities (Figure 2), and the comparison with a previous reported $[Fe^{II}Fe^{III}BPMP(OPr)_2](BPh_4)_2$[22] and $[Fe^{II}Fe^{III}BPLMP(OAc)_2](BPh_4)_2$[23].

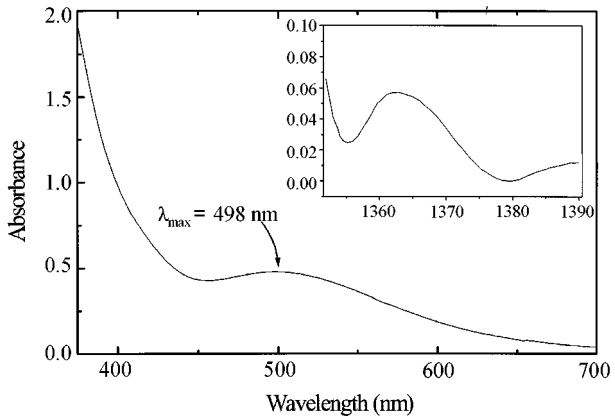

Figure 3. Visible absorption spectrum of complex **1** in CH_3CN at ambient temperature. Inset: near IR spectrum of complex **1** in CH_3CN.

All twelve CH_2 protons appear as six resonances (A_e, B_e, C_e, A_a, B_a, C_a) with very short T_1 values and two-proton integration each. The number of resonances observed suggests that there is a two-fold axis symmetry relating the two halves of the molecule. Thus, the six CH_2 resonances would arise in the half-molecule from the two protons on the phenolate backbone and the four protons associated with the pyridyl pendant arms. The COSY spectrum of complex **1** (Figure 2) shows several cross peaks of the pyridyl (β_1, γ_1, β_1') and 6-methylpyridyl (β_2, γ_2, β_2') pendants protons. However, α protons of the pyridyl ring are being very close to the metal centers. Thus, T_1 values are too short to permit its connectivity to the corresponding β protons to be observed. We assign them to remaining unassigned features with appropriately T_1 values. The CH_3 proton peak of the 6-methylpyridyl moiety is observed at -26 ppm with short T_1 value. In addition, the CH_3 protons of the bound acetate was found at 74 ppm similar to those of $[Fe^{II}Fe^{III}BPMP(OPr)_2](BPh_4)_2$[22] and $[Fe^{II}Fe^{III}BPLMP(OAc)_2](BPh_4)_2$.[23]

The analysis of the peak assignments reveals that only 16 distinct signals are observed, indicating that there is a two-fold axis symmetry relating the two halves of the molecule in the solution and the electron transfer rate between the metal centers is faster than the NMR time scale at room temperature. Therefore, complex **1** is valence-detrapped and belongs to the class II mixed-valence complex according to the Robin-Day classification.[34]

Electronic Absorption Spectra. **[**$Fe^{II}Fe^{III}BPLNP(OAc)_2](BPh_4)_2$ (**1**) is an air-stable reddish-brown solid. Complex **1** exhibits strong absorption band at 498 nm in CH_3CN ($\varepsilon = 2.6 \times 10^3\ M^{-1}cm^{-1}$) as shown in Figure 3. This band is originated from the charge transfer transition from filled $p\pi$ orbitals of phenolate oxygen to the empty $d\pi^*$ orbitals of the Fe^{III} metal center. All the previous (μ-phenoxo)mixed-valence complexes display the similar phenolate-to-Fe(III) charge transfer transition. However, complex **1** has the most blue-shifted one among the previous phenoxo-bridged mixed-valence diiron(II,III) complexes: $[Fe^{II}Fe^{III}BPMP(OPr)_2](BPh_4)_2$ (523 nm),[22] $[Fe^{II}Fe^{III}BPLMP(OAc)_2](BPh_4)_2$ (592

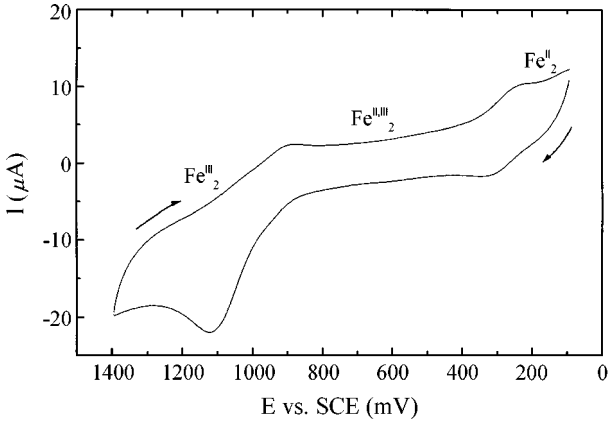

Figure 4. Cyclic voltammogram of complex **1** versus SCE in CH_3CN with 0.1 M $TBAClO_4$ under argon using a 100 mV/sec scan rate. The irreversible oxidative wave near 1000 mV is due to the oxidation of the BPh_4 counter anion.

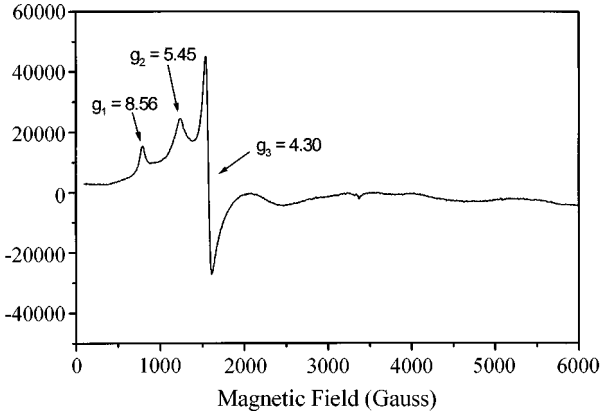

Figure 5. EPR spectrum of a frozen solution of complex **1** in CH_3CN at 4 K. Instrumental parameters: microwave frequency, 9.42 GHz; power, 5 mW; modulation frequency, 100 kHz; modulation amplitude, 5.08; gain, 2.5×10^4.

nm),[23] $[Fe^{II}Fe^{III}BIMP(OAc)_2](BPh_4)_2$ (554 nm),[24] and $[Fe^{II}Fe^{III}BZIMP(OAc)_2](BPh_4)_2$ (570 nm).[25] This is probably due to the electron-withdrawing effect of the nitro group in the bridging phenolate. Interestingly, complex **1** exhibits a broad band at 1363 nm ($\varepsilon = 5.7 \times 10^2$ $M^{-1}cm^{-1}$) in the near-IR region and this transition is similar to that of the $[Fe^{II}Fe^{III}BPLMP(OAc)_2]$ $(BPh_4)_2$ (λ_{max} = 1380 nm, $\varepsilon = 3.0 \times 10^2$ M^{-1} cm^{-1}).[23] Since defers and differed complexes do not show any near-IR bands, it can be assigned to the intervalence charge-transfer transition which is a characteristic of mixed-valence complexes.[35]

Electrochemistry. Cyclovoltammogram of complex **1** in CH_3CN is shown in Figure 4. Complex **1** displays two quasi-reversible one-electron redox processes corresponding to the $Fe^{III}_2/Fe^{II}Fe^{III}$ and $Fe^{II}Fe^{III}/Fe^{II}_2$ couples at 0.807 and 0.167 V *vs*. SCE, respectively. The first redox couple value is somewhat obscure due to the irreversible oxidative wave of the BPh_4 counter anion near 1000 mV. These values are slightly shifted to positive potential than those (0.655 and -0.085 V) of $[Fe^{II}Fe^{III}BPLMP(OAc)_2](BPh_4)_2$.[23] This anodic shift of complex **1** reflects the effect of the electron-withdrawing ability of nitro substituent of the bridging phenolate moiety.

We have determined the thermodynamic stability of the mixed-valence complex by evaluating its comproportionation constant (K_{comp}) for the equilibrium;

$$[Fe^{III}_2BPLNP(OAc)_2]^{3+} + [Fe^{II}_2BPLNP(OAc)_2]^{+} \underset{}{\overset{K_{comp}}{\rightleftharpoons}} 2[Fe^{II}Fe^{III}BPLNP(OAc)_2]^{2+} \quad (1)$$

$$\Delta E = (RT/nF) \ln K_{comp} \quad (2)$$

The large value of ΔE (0.64 V) of complex **1** yields $K_{comp} = 5.9 \times 10^{10}$ which indicates a substantial stability of the mixed-valence $Fe^{II}Fe^{III}$ complex over its corresponding Fe^{II}_2 or Fe^{III}_2 complexes. Interestingly, the comproportionation constant of complex **1** is slightly smaller than those of reported phenoxo-bridged mixed-valence complexes, $[Fe^{II}Fe^{III}BPMP(OPr)_2]^{2+}$, $[Fe^{II}Fe^{III}BPLMP(OAc)_2]^{2+}$, and $[Fe^{II}Fe^{III}BIMP(OAc)_2]^{2+}$ ($K_{comp} = 7.5 \times 10^{11}$, 3.3×10^{12}, 1×10^{11}, respectively).[22-24] The structural effects, electronic effects, and coulombic interactions are the most probable factors that determine the different stabilization for complex **1** from the comparison with $[Fe^{II}Fe^{III}BPLMP(OAc)_2]^{2+}$ and $[Fe^{II}Fe^{III}BPMP(OPr)_2]^{2+}$.[36]

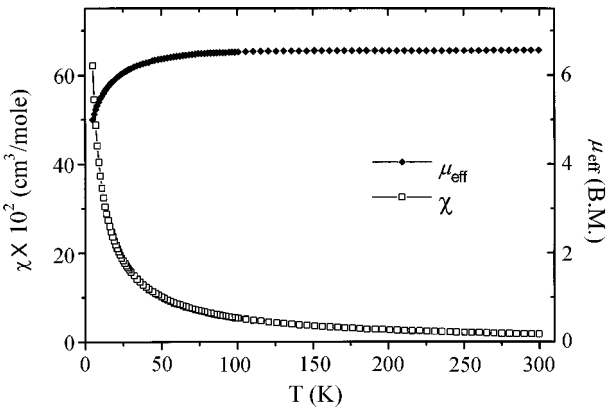

Figure 6. Plot of the magnetic susceptibility and effective magnetic moment of powder sample as a function of temperature for complex **1**. The solid line resulted form a least-squares fit of the data.

Magnetic properties. EPR spectroscopy has been very useful for characterizing the electronic and magnetic properties of the diiron(II,III) centers in the dinuclear metal complexes and proteins.[37] When the high-spin Fe^{II} ($S_1 = 2$) and Fe^{III} ($S_2 = 5/2$) centers are antiferromagnetically coupled, they exhibit characteristic signals at $g_{avg} < 2.0$ resulting from a ground state ($S_{total} = 1/2$).[38] For example, $[Fe^{II}Fe^{III}BPMP(OPr)_2]^{+}$ and $[Fe^{II}Fe^{III}BPLMP(OAc)_2]^{2+}$ complexes[22,23] exhibit broad signals near $g = 1.60$ and 1.55 due to the antiferromagnetic coupling between the two iron centers. Surprisingly, complex **1** exhibits the intense EPR signals at $g = 8.56$, 5.45, 4.30 with a very weak signals in the region of $g < 2.0$ (Figure 5). These intense signals are originated from the mononuclear high-spin Fe^{III} ($S = 5/2$) center with almost axial sym-

metry (g = 8.56, 5.45) and rhombic symmetry (g = 4.30). Thus, we can suggest that complex **1** has a very weakly antiferromagnetic coupling between the Fe^{II} and Fe^{III} center.

In order to investigate the magnetic property of complex **1**, variable-temperature magnetic susceptibility data of complex **1** in the solid state were obtained in the temperature range 5-300 K (Figure 6). The data for molar susceptibility versus temperature were fitted by using the following spin Hamiltonian:[39]

$$\boldsymbol{H} = -2JS_1 \cdot S_2 + [D_i (S_{zi}^2 - 1/3S_i(S_i+1)) + E_i (S_{xi}^2 - S_{yi}^2) + \beta S_i g_i H] \quad (3)$$

where, J is the isotropic exchange coupling constant, S_i denotes spin state (S_1 = 2 and S_2 = 5/2), and D_i and E_i are the axial and rhombic zero-field splitting parameters. The final parameter set of the fit was found to be J = -0.78 cm^{-1}, g_1 = 2.01, D_1 = -13.2 cm^{-1}, g_2 = 2.00 (fixed), and D_2 = 0.00 cm^{-1} (fixed) with E_1/D_1 = 0.15. This is quite different result from the previous $[Fe^{II}Fe^{III}BPMP(OAc)_2](BPh_4)_2$ and $[Fe^{II}Fe^{III}$-$BPLMP(OAc)_2](BPh_4)_2$ complexes that show weak antiferromagnetic couplings ($J \approx$ -5.0 cm^{-1} and J = -4.6 cm^{-1}, respectively). In addition, the observed effective magnetic moment (μ_{eff} = 6.55 BM) is slightly smaller than the value of the magnetically uncoupled high-spin Fe^{II} and Fe^{III} system (spin only value: $\mu_{eff} = [g(S_1(S_1 + 1) + S_2(S_2 + 1))]^{1/2}$ = 7.68 BM). Thus, complex **1** has a very weak antiferromagnetic coupling (J = -0.78 cm^{-1}) that is consistent with EPR data. This unusual magnetic behavior is due to the electron-withdrawing effect of the nitro group in the bridging phenolate moiety. Therefore, we can suggest that the major magnetic exchange interaction pathway between the iron centers is the oxygen atom of the bridged phenolate ligand.

Summary

We have synthesized and characterized $[Fe^{II}Fe^{III}BPLNP(OAc)_2](BPh_4)_2$ (**1**), as a new model of the reduced form of the purple acid phosphatases, in order to investigate the effect of the subtle change in the structure and electronic environment by introducing the methyl substituent on the pyridyl ring and electron-withdrawing effect of the nitro substituent on the bridged phenolate moiety.

The analysis of the NMR assignment reveals that the electron transfer rate between the iron centers is faster than the NMR time scale at room temperature. As a result, complex **1** is valence-detrapped and belongs to the class II mixed-valence complex according to the Robin-Day classification. However, complex **1** exhibits intense EPR signals at g = 8.56, 5.45, 4.30, corresponding to mononuclear high-spin Fe^{III} system. This is a very unusual feature of the mixed-valence Fe^{II}-Fe^{III} system. The magnetic susceptibility study shows a very weak antiferromagnetic coupling (J = -0.78 cm^{-1}) that is consistent with EPR data. This unusually weak antiferromagnetic coupling is due to the electron-withdrawing effect of the nitro group in the bridged phenolate moiety. Thus, we can suggest that the oxygen atom of the bridged phenolate ligand is the major pathway of the magnetic exchange interaction between the iron centers. Therefore, the dependence of the physical properties on the bridging and terminal ligand environment in the model complexes can provide important insights into the electronic and magnetic interaction of such dinuclear iron centers surrounded with hydrophobic packet amino acid residues in biological systems.

Acknowledgment. This work has been supported by the Korea University and CRM-KOSEF (2000).

References

1. For recent reviews of these enzymes, see: (a) Sanders-Loehr, J. In *Iron Carriers and Iron Proteins*; Loehr, T. M., Ed.; VCH Publishers: New York, 1989; Vol. 5, p 373. (b) Que, L., Jr.; True, A. E. *Prog. Inorg. Chem*. **1990**, *38*, 97. (c) Vincent, J. B.; Oliver-Lilley, G. L.; Averill, B. A. *Chem. Rev.* **1990**, *90*, 1447. (d) Anderson, K. K.; Gruslund, A. *Advances in Inorganic Chemistry*, **1995**, *43*, 359. (e) Wilcox, D. E. *Chem. Rev.* **1996**, *96*, 2435. (f) Strater, N.; Lipscomb, W. N.; Klabunde, T.; Krebs, B. *Angew. Chem. Int. Ed. Engl.* **1996**, *35*, 2024. (g) Klabunde, T.; Krebs, B. *Structure and Bonding* **1997**, *89*, 177.
2. Davis, J. C.; Lin, S. S.; Averill, B. A. *Biochemistry* **1981**, *20*, 4062.
3. Antanaitis, B. C.; Aisen, P. *J. Biol. Chem.* **1982**, *257*, 1855.
4. (a) Antanaitis, B. C.; Aisen, P. *Adv. Inorg. Biochem*. **1983**, *5*, 111. (b) Antanaitis, B. C.; Strekas, T.; Aisen, P. *J. Biol. Chem*. **1982**, *257*, 3766.
5. Averill, B. A.; Davis, J. C.; Burman, S.; Zirino, T.; Sanders-Loehr, J.; Loehr, T. M.; Sage, J. T.; Debrunner, P. G. *J. Am. Chem. Soc*. **1987**, *109*, 3760.
6. Dietrich, M.; Munsternmann, D.; Suerbaum, H.; Witzel, H. *Eur. J. Biochem*. **1991**, *199*, 105.
7. Kauzlarich, S. M.; Teo, B. K.; Zirino, T.; Burman, S.; Davis, J. C.; Averill, B. A. *Inorg. Chem*. **1986**, *25*, 2781.
8. Crowder, M. W.; Vincent, J. B.; Averill, B. A. *Biochemistry* **1992**, *31*, 9603.
9. Antanaitis, B. C.; Aisen, P. *J. Biol. Chem*. **1984**, *259*, 2066.
10. Lim, J. S.; Manuel, A. S.; Sykes, A. G. *Inorg. Chem*. **1996**, *35*, 614.
11. Antanaitis, B. C.; Aisen, P.; Lilienthal, H. R. *J. Biol. Chem*. **1983**, *258*, 3166.
12. Davis, S. S.; Que, L., Jr. *J. Am. Chem. Soc*. **1990**, *112*, 6455.
13. Pyrz, J. W.; Sage, J. T.; Debrunner, P. G.; Que, L., Jr. *J. Biol. Chem*. **1986**, *261*, 11015.
14. Day, E. P.; David, S. S.; Peterson, J.; Dunham, W. R.; Bonvoison, J. J.; Sands, R. H.; Que, L., Jr. *J. Biol. Chem.* **1988**, *263*, 15561.
15. True, A. E.; Scarrow, R. C.; Randall, C. R.; Holz, R. C.; Que, L., Jr. *J. Am. Chem. Soc*. **1993**, *115*, 4246.
16. (a) Lauffer, R. B.; Antanaitis, B. C.; Aisen, P.; Que, L., Jr. *J. Biol. Chem*. **1983**, *258*, 14212. (b) Scarrow, R. C.; Pyrz, J. W.; Que, L., Jr. *J. Am. Chem. Soc*. **1990**, *112*, 657. (c) Wang, Z.; Ming, L. J.; Que, L., Jr. *Biochemistry* **1992**, *31*, 5263.
17. Crans, D. C.; Simone, C. M.; Holz, R. C.; Que, L., Jr. *Biochemistry* **1992**, *31*, 11731.
18. Strater, N.; Klabunde, T.; Tucker, P.; Witzel, H.; Krebs, B. *Science* **1995**, *268*, 1489.
19. Klabunde, T.; Strater, N.; Frohlich, R.; Witzel, H.; Krebs,

B. *J. Mol. Biol.* **1996**, *259*, 737.
20. (a) Nordlund, P.; Sjoberg, B. M.; Eklund, H. *Nature* **1990**, *345*, 593. (b) Wallar, B. J.; Lipscomb, J. D. *Chem. Rev.* **1996**, *96*, 2625.
21. Suzuki, M.; Uehara, A.; Oshio, H.; Endo, K.; Yanaga, M.; Kida, S.; Saito, K. *Bull. Chem. Soc. Jpn.* **1987**, *60*, 3547.
22. (a) Borovik, A. S.; Que, L., Jr. *J. Am. Chem. Soc*. **1988**, *110*, 2345. (b) Borovik, S.; Papaefthymiou, V.; Taylor, L. F.; Anderson, O. P.; Que, L., Jr. *J. Am. Chem. Soc.* **1989**, *111*, 6183.
23. Yim, S. H.; Lee, H. J.; Lee, K.; Kang, S. J.; Hur, N. H.; Jang, H. G. *Bull. Korean Chem. Soc.* **1998**, *19*, 654.
24. (a) Mashuta, M. S.; Webb, R. J.; McCusker, J. K.; Schmitt, E. A.; Oberhausen, K. J.; Richardson, J. F.; Buchanan, R. M.; Hendrickson, D. N. *J. Am. Chem. Soc*. **1992**, *114*, 3815. (b) Mashuta, M. S.; Webb, R. J.; Oberhausen, K. J.; Richardson, J. F.; Buchanan, R. M.; Hendrickson, D. N. *J. Am. Chem. Soc*. **1989**, *111*, 2745.
25. Suzuki, M.; Oshio, H.; Uehara, A.; Endo, K.; Yanaga, M.; Kida, S.; Saito, K. *Bull. Chem. Soc. Jpn.* **1988**, *61*, 3907.
26. Borovik, A. S.; Murch, B. P.; Que, L., Jr.; Papaefthymiou, V.; Munck, E. *J. Am. Chem. Soc*. **1987**, *109*, 7190.
27. (a) Neves, A.; Erthal, S. M. D.; Drago, V.; Griesar, K.; Haase, W. *Inorg. Chim. Acta.* **1992,** *197*, 121. (b) Neves, A.; de Brito, M. A.; Vencato, I.; Drago, V.; Griesar, K.; Haase, W.; Mascarenhas, Y. P. *Inorg. Chem.* **1996**, *35*, 2360.
28. Neves, A.; de Brito, M. A.; Vencato, I.; Drago, V.; Griesar, K.; Hasse, W. *Inorg. Chim. Acta* **1993**, *214*, 5.
29. Neves, A.; de Brito, M. A.; Drago, V.; Griesar, K.; Haase, W. *Inorg. Chim. Acta* **1995**, *237*, 131.
30. Krebs, B.; Schepers, K.; Bremer, B.; Henkel, G.; Althaus, E.; Muller-Warmuth, W.; Griesar, K.; Haase, W. *Inorg. Chem*. **1994**, *33*, 1907.
31. Nie, H.; Aubin, S. M. J.; Mashuta, M. S.; Wu, C. C.; Richardson, J. F.; Hendrickson, D. N.; Buchanan, R. M. *Inorg. Chem.* **1995**, *34*, 2382.
32. Ming, L. J.; Jang, H. G.; Que, L., Jr. *Inorg. Chem.* **1992**, *31*, 359.
33. Bertini, I.; Luchinat, C. *NMR of Paramagnetic Molecules in Biological Systems*; The Benjamin/Cummings Publishing Company, Inc.: California, 1986.
34. Robin, M. B.; Day, P. *Adv. Inorg. Chem. and Radiochem*. **1967**, *10*, 247.
35. Creutz, C. *Prog. Inorg. Chem*. **1983**, *30*, 1.
36. Gagne, R. R.; Spiro, C. L.; Smith, T. J.; Hamann, C. A.; Thies, W. R.; Shuemke, A. K. *J. Am. Chem. Soc*. **1981**, *103*, 4073.
37. Wertz, J. E.; Bolton, J. R. In *Electron Spin Resonance: Elementary Theory and Practical Applications*; McGraw-Hill, Inc.: 1972.
38. Munck, E.; Debrunner, P. G.; Tsibris, J. C. M.; Gunsalus, I. C. *Biochemistry* **1972**, *11*, 855.
39. Day, E. P.; Kent, T. A.; Lindahl, P. A.; Münck, E.; Orme-Johnson, W. H.; Roder, H.; Roy, A. *Biophys. J*. **1987**, *52*, 837.